Fine structure of Rydberg states. V. $n=5$ and $6F$ and G states of ^{4}He

John W. Farley,* Doreen A. Weinberger, Shin-Sheng Tarng, Nancy D. Piltch, and William H. Wing
Physics Department and Optical Sciences Center, University of Arizona, Tucson, Arizona 85721
(Received 27 August 1981)

We have made 17 new high-precision measurements of the nF-nG intervals ($n=5,6$) of neutral ^{4}He using the microwave-optical method. The rms one-standard-deviation experimental uncertainty for the transitions reported here is 188 kHz (14 ppm). The new measurements agree with the predictions of a least-squares fit to previous experimental data, and are up to 40 times more precise. The nF-nG manifold is now known experimentally to better than 1 MHz for all values of the quantum numbers. The precision of the experimental measurement exceeds that of the best currently available theory by approximately three orders of magnitude.

I. INTRODUCTION

The helium atom is of interest from the point of view of fundamental atomic physics because it is the simplest multielectron system. In addition, helium plays an important role in a variety of laboratory and astrophysical plasmas. The ^{4}He isotope is composed of two electrons bound to a doubly charged spinless nucleus. The atom in a singly excited Rydberg state is composed of a single valence electron loosely bound to a hydrogenic core. Helium has long been the subject of theoretical interest; calculations of its structure played an important role in the development of quantum theory. In view of both the long history of interest in the subject and the simplicity of the three-body system, one might expect theory and experiment to be in excellent agreement. However, this is not the case: The precision of the experimental measurements often exceeds that of the best currently available theory by several orders of magnitude. Evidently this is a standing challenge to the theoretical physics community and a natural test case for the development of many-body calculational techniques and high-precision perturbation theory.

Over the past decade, our group has carried out a series of high-precision measurements on the fine structure (fs) of highly excited states of ^{4}He.[1-7] In Ref. 4, the method was summarized and the basic apparatus described. Measurements were reported of $n=6$ and 7 D-F intervals. In Ref. 5, results in $n=8$, 9, and 16–18 were reported, and empirical formulas useful in predicting the position of unmeasured members of the series were given. Reference 6 reported measurements in $n=6$, 7, 9–12, and 16. Two-quantum resonances were observed with an improved apparatus, and the first precision measurements of fs in G states ($L=4$) were reported. The most recent publication, by Farley, MacAdam, and Wing,[7] (FMW) reported the results of an extensive measurement program carried out with an automated apparatus.[8] We reported 67 new measurements in $n=6-11$ D, F, and G states. The new data approximately doubled the number of high-precision measurements in D-F-G states of ^{4}He.

Since our last publication, there have been two high-precision experimental studies of Rydberg states of ^{4}He by other groups. Cok and Lundeen[9] (CL) applied the Ramsey separated oscillatory field technique in the 2–4 GHz microwave band to a fast neutral beam produced by collisional charge-exchange neutralization of an ion beam. They obtained measurements of the intervals in the states with $n=7-8$, $L=3-6$. The uncertainties of their measurements are comparable to our own. Secondly, Panock *et al.*[10] and Rosenbluh *et al.*[11] made measurements using the motional Stark effect spectroscopic technique, in which a large magnetic field is used to Zeeman tune an atomic transition into resonance with the radiation from a CO_2 or molecular FIR laser. The motional electric field experienced by the atoms results in an interesting asymmetric line shape. In addition, the electric field mixes the states, allowing the observation of normally forbidden transitions. Both these effects were in fact exhibited about a decade ago in microwave spectra taken during the early stages of our own research program,[2] but were not used for

precise spectroscopy. In Ref. 10, transitions from the 7^1S state to the 9^1L ($L=0-8$) state were observed. In Ref. 11, measurements were made of five intervals among S and P states ($n=7-9$) whose frequencies fell in the range $67-980$ cm^{-1} ($2\times10^3-3\times10^4$ GHz). The precision was 6–12 MHz (0.2–6 ppm).

In addition to these studies of ^{4}He, several recent experiments have signaled a revival of interest in ^{3}He, whose spectrum is complicated by the presence of hyperfine structure (hfs). Lawler *et al.*[12] used a tunable dye laser to drive the 2^3P-3^3D transition at 587.5 nm. They employed Doppler-free saturation spectroscopy with the intermodulated optogalvanic detection technique. Optical resonances induced in a dc helium discharge were detected as changes in the discharge current. Three hfs intervals of the 3^3D state were measured with uncertainties of 0.8–6 MHz. Giacobino *et al.*[13] employed a cw dye laser and two-photon excitation to drive the 2^3S-4^3D transitions in a pulsed discharge. In order to enhance the optical electric field, the cell was placed in a Fabry-Perot cavity. The resonance was detected by monitoring the fluorescence. Four hfs intervals in the 4^3D state were measured with uncertainties of 3–5 MHz. Freeman *et al.*[14] measured the isotope shift of the 2^3P-3^3D line at 587.5 nm using the same technique employed by Lawler *et al.* Derouard *et al.*[15] observed anticrossing resonances in the nD states ($n=3-6$) of ^{3}He. The hfs induces resonances between the singlet and triplet states. The singlet-triplet intervals were measured with uncertainties of 5–20 MHz (49–1000 ppm). The ^{3}He/^{4}He isotope shift in the singlet-triplet splitting is larger than expected on the basis of theory, by roughly a factor of 20. Derouard *et al.* attributed this effect to hfs-induced configuration interaction.

Two other related papers deserve mention. Tam[16] reviewed several experimental measurements of the relativistic structure of the 3^3P state. In a recent theoretical work, Cok and Lundeen[17] assessed the adequacy of the present theoretical understanding of the structure of the Rydberg helium manifold.

In FMW, we performed a least-squares fit to all existing state-resolved data, using a plausible empirical fitting formula with adjustable coefficients. With the optimized coefficients in hand, we took advantage of regularities of the Rydberg series in order to extrapolate confidently upward toward the ionization limit, predicting the intervals for high-lying unmeasured members of the manifold. The same formula also yields values for the low-lying members of the manifold. However, the extrapolation procedure is somewhat less reliable in this case because the variation of the quantum defect with n becomes more pronounced for low values of n. We concluded in FMW that the structure of the D-F-G manifold of ^{4}He was known to a precision of 1 MHz or better, except for a few transitions for which the principal quantum number n is 6 or less.

Since the publication of FMW, we have performed new measurements in $n=5$ and 6 F and G states. Since the $5G$ state is the lowest possible G state, the new measurements complete the spectroscopy of F-to-G transitions. In this paper, we discuss the experimental arrangements and present our new results. The experimental results are compared with estimates extrapolated from measurements of states with higher values of n. Several statistical studies of the data are described. We conclude with a brief assessment of the current status of the theory.

II. APPARATUS

The microwave-optical method, the experimental technique employed here, has been described elsewhere[3] and will only be sketched briefly. Figure 1 is a schematic representation of the technique. Rydberg states are produced in a low-pressure sample of helium, which is excited by electron bombardment with a simple electron gun. The populations of the Rydberg states are monitored by measuring the intensity of an atomic emission line with a monochromator and a photomultiplier tube. The helium sample is subjected to a weak microwave field, whose frequency is varied. When the microwave frequency matches an appropriate interval in the Rydberg manifold, the microwave electric field drives electric-dipole transitions between the corresponding Rydberg states. The resulting alteration of the populations produces a change in the intensity of the atomic emission line. Hence a resonance induced in the microwave regime is detected in the optical regime, with enhanced sensitivity and resolution. Because the Doppler width scales in proportion to the frequency and is less than the natural radiative linewidth at microwave frequencies, the method is effectively Doppler free. The spectrometer has been automated by interfacing it to an S-100 bus "personal" microcomputer. Details of the automation have been given elsewhere.[8]

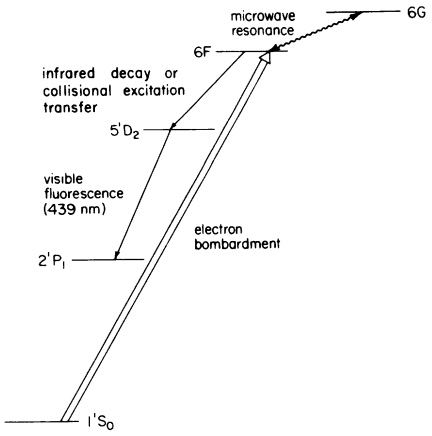

FIG. 1. An example of the excitation and detection scheme employed in the experiments reported here (not to scale). Rydberg $6F$ and $6G$ states (for example) are excited from the ground state by electron bombardment. Microwave resonances near 8.8 GHz are induced between the F and G states. The F and G state populations evolve by collision or infrared radiative decay to the 5^1D_2 state. The D state in turn decays to the 2^1P_1 state with the emission of visible radiation. The F-G microwave resonance is detected as a change in the intensity of the 5^1D_2-2^1P_1 atomic emission line as a function of the microwave frequency. Individual levels of the F and G manifold are resolved in the experiments but are not displayed separately in this figure.

A variation of the standard procedure was employed in this work. The atomic emission lines from the states involved could not be monitored because their wavelengths are in the infrared, where conventional photomultiplier tubes do not respond. Nor could other infrared detectors be employed, because the blackbody radiation from the hot ($T\sim 1400$ K) electron-gun cathode masked the relatively feeble atomic emission. Instead, the resonances were monitored indirectly: the population of the Rydberg state was transferred by radiative decay, blackbody radiation excitation, or collision to a different state, whose emission line was in the technically convenient blue or near-ultraviolet region of the spectrum. The signal thus observed is proportional to the difference of the transfer rates from the two resonating states to the fluorescing state. The difference may be small, particularly for collisional transfer, and hence the signal intensity is generally weaker than in direct detection. The atomic emission lines used for detection and the nominal microwave transition frequencies for the new measurements are listed in Table I. The radiative transfer rates (both spontaneous and stimulated) between the $6F$ and $6D$ states demonstrate that collisional excitation transfer is clearly the dominant mechanism contributing to signals observed in the $6D$-$2P$ fluorescence.

The Grotrian diagram of the energy levels involved in the F-G microwave resonances are shown in Fig. 2. The spin-orbit interaction is sufficiently strong that the two levels with the same values of J are strongly coupled. All states either are pure triplet or have substantial triplet character. Consequently there are no rigorous spin selection rules applicable to electric-dipole transitions. The only selection rules are the restriction of the changes in the orbital angular momentum L to unity and in the total angular momentum J to unity or zero. These yield 11 possible transitions in the F-G manifold.

In a typical resonance scan, the microwave frequency was stepped through approximately 20 points in an interval of 10 MHz, approximately centered on the transition. The typical raw count rate was several hundred kHz. Total integration time for an individual run varied from 1—24 h, with a typical value of 2—6 h. A typical value for the signal-to-noise ratio was 10. The helium pressure was varied between 1×10^{-3} and 5×10^{-3} Torr. The electron beam current was approximately 1 mA through an area of roughly 1 cm^2. The electron beam voltage was varied between 30 and 200 V.

III. RESULTS

The results of our measurements are summarized in Table II. The uncertainties shown are one standard deviation (1SD) error bars. The procedure employed in the search for systematic errors was identical to that of FMW and need not be described. No systematic errors were found to be significant at our level of sensitivity. Room-temperature blackbody radiation can shift resonances, but a calculation of the magnitude of this effect for these states of helium[18] yields less than 1 kHz, and we therefore neglected it and merely averaged over the 3—13 resonance runs for a given transition. The results reported in Table II represent 138 individual resonance runs comprising 655 h of data-taking time.

There is one ambiguity in the assignment of quantum numbers. A resonance was observed at 8959.533 ± 0.117 MHz, which is a blend of the unresolved 6^3F_4-6^3G_5 and 6^3F_3-6^3G_4 resonances. The splitting predicted by the preliminary fit (discussed in Sec. IV) is only 778 kHz. Since the resonances overlap within their natural widths, we have noted

TABLE I. Nominal microwave intervals, sources, typical power levels, and optical transitions monitored. The particular optical transition monitored depended on the individual microwave transition; some microwave transitions were seen on up to four optical lines.

Microwave transition group	Nominal microwave interval (GHz)	Microwave source	Nominal power level (μW)[a]	Optical transition monitored (nm)
6*F*-6*G*	15	HP8620C programmable sweep generator	100	6^1D-2^1P (414) 5^1D-2^1P (439) 4^1D-2^1P (492) 6^3D-2^3P (382) 5^3D-2^3P (403) 4^3D-2^3P (447)
5*F*-5*G*	9	Varian VA290C klystron	500	4^1D-2^1P (492) 4^3D-2^3P (447)

[a]Microwave power level was varied from run to run in a search for systematic errors. The listed power level is the flux through an area of approximately 10 cm^2. There remains an uncertainty of perhaps a factor of 2 due to calibration errors, transmission losses, etc.

the resonance in a footnote to Table II, but have excluded this datum as a precision measurement.

One resonance which was not found in either $n=5$ or $n=6$ was the $n\,^3F_4$-$n\,^3G_3$ transition. Nor was it reported in $n=8$ by CL. This resonance was not observed because the angular momentum factors in the transition matrix element are very small for this particular transition. The microwave power level required to saturate is 2 or 3 orders of magnitude higher than the levels required for other resonances in the same transition group. Such a high power level would broaden and shift the stronger resonances into the weak one, rendering a meaningful measurement impossible.

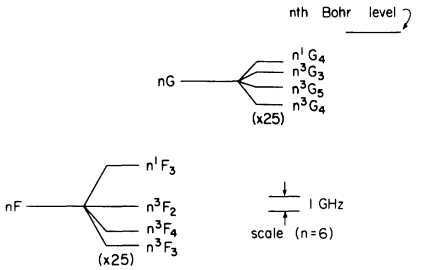

FIG. 2. Structure of the *nF*-*nG* energy level manifold, drawn to scale. The expanded scale shows the details of the triplet states. The spin-orbit interaction couples the two levels with the same value of the total angular momentum J. The two levels repel each other, driving the $^3F_3$ level below the $^3F_4$ level and similarly the $^3G_4$ level below the $^3G_5$ level. This is in contrast to the cases of the triplet P and triplet D states, where the singlet-triplet repulsion is relatively less important, and the sublevels form normal "inverted triplets" with the state of highest J at lowest energy. For F and G states, the singlet and triplet designations are conventional rather than exact; every state has substantial triplet character. Consequently, the only effective selection rule for F-to-G electric-dipole transitions restricts the change in J to zero or unity, yielding 11 possible transitions.

Also listed in Table II are two earlier experimental measurements of the 6^1F_3-6^1G_4 transition from previous publications by our group. The difference between new and old measurements of this interval is 1.16 combined standard deviations in one case[6] and 0.12 combined standard deviations in the other.[7] A measure of the overall agreement among the three measurements can be obtained from the total χ^2 of 1.40 (2 degrees of freedom). There is a 50% chance of obtaining a value of χ^2 this large by chance.

IV. DISCUSSION

We have performed least-squares fits to experimental data, using procedures described in detail in FMW. Only the outline is given here. Each energy level is modeled by the formula

$$E(n,L,S,J)=\frac{A(L,S,J)}{n^3}+\frac{B(L,S,J)}{n^5}+\frac{C(L,S,J)}{n^7}\,. \tag{1}$$

TABLE II. High-precision experimental measurements of $n=5$ and 6 F-G intervals. All of the experimental measurements are from this work unless specifically noted otherwise. The intervals are listed in order of the energy of the states involved, with the lowest-energy state listed first. Uncertainties listed are 1SD error bars. We also list the best previous value for the intervals, the "preliminary fit," a least-squares fit to previous experimental data. We also list the results of the "final fit," a least-squares fit to all state-resolved experimental D-F-G data, including the new measurements reported here. The variable z_{PF} measures the agreement between preliminary fit and the experimental datum; z_{FF} does the same for the final fit. They are discussed in detail in Sec. IV of the test.

	Measured transition frequency (MHz)	Number of runs	Reduced χ^2	Preliminary fit (MHz)[a]	z_{PF}	Final fit (MHz)[b]	z_{FF}
5^3F_3-5^3G_4	c			14 891.491±3.513		14 889.192±0.418	
5^3F_3-5^3G_3	15 049.142±0.145	5	1.8	15 049.179±4.380	0.0084	15 048.474±0.275	−2.15
5^3F_3-5^1G_4	15 100.035±0.465	3	5.1	15 100.014±2.268	−0.0091	15 098.873±0.421	−1.85
5^3F_4-5^3G_4	14 797.994±0.150	6	1.7	14 798.428±4.960	0.087	14 797.604±0.258	−1.31
5^3F_4-5^3G_5	14 877.846±0.211	6	2.6	14 876.949±6.013	−0.149	14 877.826±0.463	−0.04
5^3F_4-5^3G_3	c			14 956.117±5.446		14 956.886±0.392	
5^3F_4-5^1G_4	15 007.343±0.098	3	0.92	15 006.951±4.139	−0.095	15 007.285±0.199	−0.26
5^3F_2-5^3G_3	14 824.668±0.310	6	2.0	14 827.743±5.244	0.585	14 823.606±0.569	−1.64
5^1F_3-5^3G_4	14 511.933±0.142	13	1.7	14 518.055±3.398	1.800	14 512.527±0.262	1.99
5^1F_3-5^3G_3	14 670.769±0.172	10	3.9	14 675.744±4.282	1.161	14 671.809±0.302	2.99
5^1F_3-5^1G_4	14 721.426±0.265	9	1.8	14 726.578±2.078	2.095	14 722.209±0.300	1.96
6^3F_3-6^3G_4	d			8 959.640±0.517		8 959.892±0.136	
6^3F_3-6^3G_3	9 051.505±0.070	12	2.92	9 051.076±0.937	−0.457	9 051.684±0.106	1.41
6^3F_3-6^1G_4	9 080.412±0.150	8	1.94	9 080.544±0.195	1.864	9 081.024±0.123	3.15
6^3F_4-6^3G_4	8 911.773±0.064	9	1.61	8 911.131±1.131	−0.567	8 911.794±0.104	0.17
6^3F_4-6^3G_5	d			8 957.977±1.456		8 959.114±0.274	
6^3F_4-6^3G_3	c			9 002.566±1.315		9 003.585±0.138	
6^3F_4-6^1G_4	9 032.560±0.073	12	1.88	9 032.035±1.012	−0.517	9 032.926±0.099	2.98
6^3F_2-6^3G_3	8 926.163±0.132	5	0.84	8 927.212±1.233	0.846	8 926.833±0.188	2.92
6^1F_3-6^3G_4	8 732.980±0.075	9	1.39	8 733.081±0.488	0.205	8 732.676±0.095	−2.51
6^1F_3-6^3G_3	8 824.635±0.058	13	2.33	8 824.517±0.917	−0.128	8 924.467±0.098	−1.48
6^1F_3-6^1G_4	8 854.098±0.104 8 853.965±0.050[e] 8 854.062±0.270[f]	9	2.08	8 853.985±0.078	−0.869	8 853.807±0.079	−2.23

[a]Results of a least-squares fit to all but one of the experimental measurements in Table IV of Ref. 7 and the 8F-8G transitions reported in Ref. 9.

[b]New least-squares adjustment. The input-data set consists of the data described in note a and the new measurements in this table.

[c]This transition was not observed.

[d]A resonance was observed at 8959.533±0.117 (7 runs, reduced χ^2 of 2.77). It could be attributed to either of the 6^3F_3-6^3G_4 or 6^3F_4-6^3G_5 transitions, which are unresolved, or to a blend of the two with unknown weights.

[e]Farley, MacAdam, and Wing, Ref. 7.

[f]MacAdam and Wing, Ref. 6.

A transition frequency ν is given by the difference of two such expressions:

$$\nu = E(n,L,S,J) - E(n,L',S',J') .$$

$E(n,L,S,J)$ represents in frequency units the displacement of an energy level from the energy-reference level, arbitrarily chosen to be the n^3G_5 state. A, B, and C are empirical constants, which are adjusted to give the best fit to the experimentally measured transition frequencies.

The A coefficient of Eq. (1) is closely related to the quantum defect. This can be derived by examining an approximate expression for the binding energy, valid for high values of n.

$$-Rhc/(n-\delta)^2 \simeq -Rhcn^{-2} - 2Rhc\delta n^{-3} . \quad (2)$$

Here R is the Rydberg constant and δ is the quantum defect. The first term on the right is the energy of the Bohr level. Comparison of the second term on the right with Eq. (1) indicates that to first approximation $A \simeq -2Rc\delta$. No fundamental significance should be attached to the choice of exponents in the higher-order terms of Eq. (1). In FMW, we discussed alternative forms of Eq. (1), in which the n^{-7} term was replaced by n^{-k}. Equally good fits were obtained for $k=4$, 6, or 7.

The quantity minimized in the fit is the reduced χ^2, given by

$$\chi^2 = \frac{1}{f} \sum_{i=1}^{N} \frac{(\nu_i - \nu_F)^2}{\sigma_i^2} . \quad (3)$$

Here ν_i and σ_i are the ith experimental value and the 1SD uncertainty, respectively, ν_F is the fitted value, f is the number of degrees of freedom, and i ranges over the entire data set.

We have performed least-squares fits, using Eq. (1), on two distinct input data sets. The first data set consists of all but one of the high-precision experimental data of Table IV of FMW (138 data) and 10 data in the $n=8$ F-G transition group from CL. The excluded datum is an old measurement of the 5^3F_3-5^3F_4 interval, which is clearly in error, from Ref. 22 of FMW. The new measurements reported here, however, are excluded. We refer to this data set and the resulting fit as the preliminary data set and the preliminary fit. The second data set consists of all the data in the preliminary data set and the 17 new measurements as well. We refer to these as the final data set and the final fit. The uncertainties attached to both of the fits were extracted using the variance-covariance matrix via standard statistical formulas.

The preliminary fit was used to guide the initial search for the resonances. In the search for weak resonances, the accuracy of initial estimates of the resonance frequencies was a crucial factor contributing to success. The uncertainties in the results of the preliminary fit reflect both errors in the experimental data base and model errors (e.g., omission of higher-order terms in the fitting formula). Since Eq. (1) is a power series in inverse powers of the principal quantum number n, the preliminary data set, containing measurements from high values of n, determines the coefficients of the lower-order terms of the formula better than the coefficients of the higher-order terms. At lower values of n, however, it is the poorly known higher-order terms which become relatively more important. Consequently, the results of the preliminary fit have larger uncertainties for lower values of n. The utility of the new measurements reported here is then twofold: first, they serve as a stringent test of the accuracy of the preliminary fit; secondly, because the new data are considerably more precise than the results of the preliminary fit, they form part of the final data set, which enables us to determine the high-order coefficients accurately.

The final fit serves to smooth out random errors in the data. Consequently, the predictions of the final fit are more reliable than the raw data themselves. Figure 3 displays the uncertainties in the n^3F_4-n^3G_5 transition for $n=5-15$ returned by the preliminary fit and the final fit. The results are typical of F-G transitions. We see that the inclusion of the new measurements in the input-data set results in dramatic reductions in the uncertainties for $n<7$. Our new experimental measurements are most valuable in probing the structure of the lower excited states, which penetrate more deeply into the core.

We obtain a quantitative measure of the extent of agreement between the preliminary or final fit, on the one hand, and the new data, on the other, in two ways. First, we examine the fit by comparing the values of the preliminary or final fit with the new data. This is a "local" test, because the comparison is confined to the transitions for which new data are available. Second, we perform a "global" test by examining how the inclusion of the new measurements affects the overall goodness of the fit.

To carry out the local test, we define the dimensionless variables z_{PF} and z_{FF}:

$$z_{\mathrm{PF}} = (\nu_{\mathrm{PF}} - \nu_{\mathrm{expt}})/(\sigma_{\mathrm{PF}}^2 + \sigma_{\mathrm{expt}}^2)^{1/2} , \quad (4)$$

$$z_{\mathrm{FF}} = (\nu_{\mathrm{FF}} - \nu_{\mathrm{expt}})/(\sigma_{\mathrm{FF}}^2 + \sigma_{\mathrm{expt}}^2)^{1/2} . \quad (5)$$

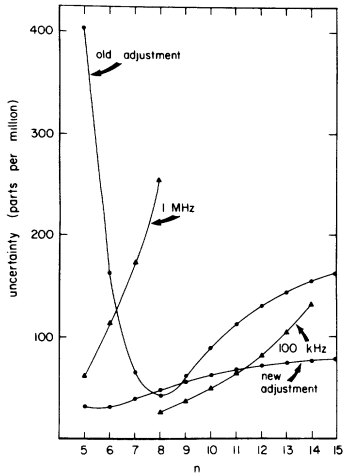

FIG. 3. The uncertainties in the n^3F_4-n^3G_5 intervals returned by two least-squares fits to experimental data are shown as a function of the principal quantum number n. The input data set for old adjustment (the "preliminary fit") excludes the new measurements reported here, while the input data set for the new adjustment (the "final fit") includes them. The most marked improvement for the uncertainties is achieved for low values of the principal quantum number n ($n<7$).

Here ν_{PF} is the value returned by the preliminary fit, ν_{FF} is the value returned by the final fit, and ν_{expt} is the new experimental measurement. The associated 1SD uncertainties are indicated by the symbol σ with the appropriate subscript. If there is agreement between the preliminary (final) fit and the new experimental data, z_{PF} (z_{FF}) will have a Gaussian distribution with a mean of zero and a standard deviation of unity.

Examination of Table II shows that agreement between the new data and the preliminary fit is very satisfactory. The rms value of z_{PF} is 0.945, compared with a theoretically expected value of unity. In 13 of 17 cases (76%), agreement was within 1SD, whereas statistically one expects this level of agreement in 12 cases (68%). At the 2SD level, agreement was achieved in 16 of 17 cases (94%), which is the statistically expected number. The worst case differs by 2.1 combined standard deviations. By this measure, the data is evidently under good statistical control. This means that the combined standard deviation in Eq. (4) realistically reflects the differences between experiment and fit. Since the dominant contribution comes from σ_{PF}, we conclude that the uncertainties σ_{PF} returned by the preliminary fit are realistic. In contrast, no conclusion can be drawn from this about whether the experimental uncertainties σ_{expt} assigned to the

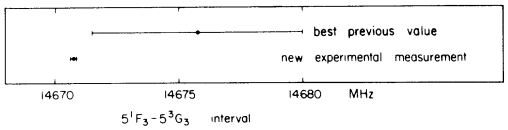

FIG. 4. Values for the 5^1F_3-5^3G_3 interval. Our new measurement is shown, as well as the best previous value for the interval, an extrapolation from measurements of states at higher values of n (referred to in the text as the "preliminary fit").

new measurements are realistic, because they make only a small contribution to the combined standard deviation.

The new measurements are not only in agreement with the preliminary fit; they are also more precise, as comparison of σ_{expt} with σ_{PF} in Table II shows. For the $n=6$ data, the rms 1SD uncertainty improved from 853 to 96 kHz, nearly a factor of 9. For the $n=5$ data, the rms uncertainty decreased from 6.09 to 0.243 MHz, a factor of 25. For the entire set of new measurements, the rms uncertainty decreased from 4.46 MHz to 188 kHz, a factor of 24. The improvement achieved for a typical case, the 5^1F_3-5^3G_3 transition, is displayed graphically in Fig. 4.

The extent of agreement between the final fit and the new data may be judged by the values of z_{FF}. If the data are under good statistical control, z_{FF} will be normally distributed with zero mean and standard deviation of unity. Values for z_{FF} for each datum are listed in the last columm of Table II. The rms value of z_{FF}, averaged over the new data, is 2.06. This is fairly large: there is less then a 4% chance of obtaining a figure this large by chance. Hence there is marginal disagreement between the final fit and the new data.

Further insight is provided by examining the overall goodness of the least-squares fit for different input-data sets. The reduced χ^2 is a figure of merit, reflecting the goodness of fit over the entire data set, whereas the variables z_{PF} and z_{FF} range only over the set of new measurements. The preliminary fit gives a reduced χ^2 of 2.52 (121 degrees of freedom), whereas the final fit gives a reduced χ^2 of 4.86 (138 degrees of freedom). Hence the new fit is significantly worse than the old.

A perfect model, with correctly estimated uncertainties, would yield a reduced χ^2 of unity. In FMW, we concluded that both underestimation of experimental uncertainties and model error [for example, omission of higher-order terms in Eq. (1)] contributed comparable amounts to the excess reduced χ^2. Both factors are presumably operative

in the new measurements.

The increase of χ^2 indicates a relatively poorer fit which can be attributed to an intensification of the two underlying causes. Either the new measurements underestimate the experimental uncertainties by more than the old measurements did, or the model is more inaccurate at low n, or both. There are reasons to believe that both factors contribute to some extent. The new resonances are weak, with signal-to-noise poorer than typically found in the old measurements. Hence, the observed resonance signal may be distorted by other weak overlapping resonances cascading into the same emission line. The second source of inaccuracy, increased model error at low values of n, is expected to play a role because the formula is a power series in inverse powers of n. This may indicate that more terms are needed in the present form of the fitting formula.

There are other types of model error, of course. A different form of the fitting formula might yield better results. For example, the expression for the energy might involve the effective quantum number n^* rather than n, by analogy with the well-known examples of fine-structure intervals in alkali-metal atoms, which scale in proportion to $(n^*)^{-3}$ rather than n^{-3}. Such an expression would, however, be impractical. Because our experiments measure transitions between states of the same values of n, we cannot determine the absolute magnitude of quantum defects, but only expressions related to the difference of quantum defects. Consequently, we use the integral n rather than the less-well-determined n^*. In helium D-F-G states, because the quantum defects are much smaller than those of alkali-metal atoms, n^* is equal to n to a good approximation. The errors arising from this procedure are presumably absorbed in the coefficients of the higher-order terms of Eq. (1).

V. CONCLUSION

With this paper, we have extended our measurement program down to the lowest members of the F-G series. The structure of the nF-nG manifold is now known to better than 1 MHz for all values of n. Hence the spectroscopy of the F-G manifold of ^{4}He is now complete. At the level of precision of a few MHz, the remaining incompletely explored territory of the ^{4}He spectrum consists of a few relativistic intervals in the $4F$ state (whose uncertainties are $\lesssim 3$ MHz), intervals in the nD states ($n=3-6$), intervals in the S and P states (which have been the subject of some recent measurements[10,11]), and the states for which $L>4$ (which have been the subject of studies by Beyer and Kollath[19] and by Cok and Lundeen[9]). Despite the pioneering work of Fred *et al.*[20] and Descoubes,[21] and the more recent work discussed in Sec. I, the high-precision investigation of the ^{3}He isotope has scarcely begun.

The accuracy of the best available theoretical calculation lags considerably behind that achieved by experiment. A recent assessment of the status of the theory by Cok and Lundeen[17] reached essentially the same conclusion as FMW: the theoretical accuracy is of the order of 1% for a typical (30 GHz) interval, while the experimental figure is 3 orders of magnitude better. There have been rather few efforts in recent years to close the gap. The relative lack of theoretical effort in helium, compared to the situation in hydrogen, is quite striking. No doubt the reason for the "quiet on the helium front" has been that, until recently, there was a dearth of high-precision data for meaningful comparisons. In view of helium's role as the simplest atomic system for which an exact solution is unavailable in either the nonrelativistic or Dirac approximation, a renewed theoretical effort is desirable.

ACKNOWLEDGMENTS

This work has been supported in part by the National Science Foundation under Grant No. PHY 79-15302. One of us (W. H. W.) gratefully acknowledges the kind hospitality of the Joint Institute for Laboratory Astrophysics, University of Colorado and National Bureau of Standards, Boulder; the Massachusetts Institute of Technology, Cambridge; the École Normale Supérieure, Paris; and the support of the John Simon Guggenheim Memorial Foundation during the course of this investigation.

*Present address: Department of Physics, University of Oregon, Eugene, Oregon 97403.

[1]W. H. Wing and W. E. Lamb, Jr., Phys. Rev. Lett. 28, 265 (1972).

[2]W. E. Lamb, Jr., D. L. Mader, and W. H. Wing, in *Fundamental and Applied Laser Physics, Proceedings of the Esfahan Symposium,* edited by M. S. Feld, A. Javan, and N. A. Kurnit (Wiley, New York, 1973), pp. 523—538; W. H. Wing, K. R. Lea, and W. E. Lamb, Jr., in *Atomic Physics 3,* edited by S. J. Smith and G. K. Walters (Plenum, New York, 1973), pp. 119—141.

[3]W. H. Wing and K. B. MacAdam, in *Progress in Atomic Spectroscopy,* edited by W. Hanle and H. Kleinpoppen (Plenum, New York, 1978), pp. 491—527.

[4]K. B. MacAdam and W. H. Wing, Phys. Rev. A 12, 1464 (1975).

[5]K. B. MacAdam and W. H. Wing, Phys. Rev. A 13, 2163 (1976).

[6]K. B. MacAdam and W. H. Wing, Phys. Rev. A 15, 678 (1977).

[7]J. W. Farley, K. B. MacAdam, and W. H. Wing, Phys. Rev. A 20, 1754 (1979), referred to in the text as FMW.

[8]J. W. Farley, A. H. Johnson, and W. H. Wing, J. Phys. E 13, 848 (1980).

[9]David R. Cok and S. R. Lundeen, Phys. Rev. 23, 2488 (1981), referred to in the text as CL.

[10]R. Panock, M. Rosenbluh, B. Lax, and Terry A. Miller, Phys. Rev. A 22, 1050 (1980).

[11]M. Rosenbluh, Han Le, B. Lax, R. Panock, and Terry A. Miller, Opt. Lett, 6, 99 (1981).

[12]J. E. Lawler, A. I. Ferguson, J. E. M. Goldsmith, D. J. Jackson, and A. L. Schawlow, Phys. Rev. Lett 42, 1046 (1979).

[13]E. Giacobino, E. de Clerc, F. Biraben, G. Grynberg, and B. Cagnac, in *Laser Spectroscopy IV,* edited by H. Walther and K. W. Rothe (Springer, Berlin 1979).

[14]R. R. Freeman, P. F. Liao, R. Panock, and L. M. Humphrey, Phys. Rev. A 22, 1510 (1980).

[15]J. Derouard, M. Lombardi, and R. Jost, J. Phys. (Paris) 41, 819 (1980).

[16]A. C. Tam, Phys. Rev. A 20, 1784 (1979).

[17]D. R. Cok and S. R. Lundeen, Phys. Rev. A 19, 1830 (1979).

[18]J. W. Farley and W. H. Wing, Phys. Rev. A 23, 2397 (1981).

[19]H. J. Beyer and K. J. Kollath, J. Phys. B 11, 979 (1978).

[20]M. Fred, F. S. Tomkins, J. K. Brody, and M. Hamermesh, Phys. Rev. 82, 406 (1951).

[21]J. P. Descoubes, in *Physics of One- and Two-Electron Atoms,* edited by F. Bopp and H. Kleinpoppen (North-Holland, Amsterdam, 1969), pp. 341—347.